

On the applicability of quantitative infrared thermography on window glazing

Kim Carbonez, M.Sc.¹

Nathan Van Den Bossche, Assistant Professor¹

Marijke Steeman, Assistant Professor¹

Sven Van De Vijver, MEng.¹

Arnold Janssens, Full Professor¹

¹ Ghent University, Belgium

KEYWORDS: *infrared thermography, glazing, quantitative analysis, U-value,*

SUMMARY

Energy efficient buildings are an essential factor to reduce the energy consumption by 2020. New buildings have to meet severe requirements, whereas older buildings need renovation to reduce the heat losses through the building envelope. Infrared thermography (IRT) might be an improvement over existing methods to assess the thermal performance of an existing wall in a non-destructive way, or to check upon the as-built quality, specifically in the case of window glazing. The technique instantly visualises the surface temperature of a whole building part, and in turn might allow to deduce the thermal transmittance accordingly. However, many parameters can influence the surface temperature and lead to distorted conclusions. This paper reports on the impact of different indoor and outdoor boundary conditions for the assessment of the U-value of glazing, using the results from a numerical simulation model. After an analysis of 6 types of windows, it is concluded that for specific conditions, IRT might allow to estimate the U-value with an acceptable accuracy, based upon the instantaneous indoor surface temperature. In future research, experiments will be performed to validate this conclusion and the assessment methodology will be improved.

1. Introduction

Energy efficiency and sustainability are major concerns of our time. In 2011, the European Commission decided that the energy consumption in general should decrease with 20% by 2020 (compared to 1990) (EC, 2011). To reach this goal, the building industry has to comply with stringent regulations in respect to insulating performance, airtightness quality, renewable energy sources, etc. However, new buildings only constitute a minority of the building stock. In Belgium, 62 % of the buildings have been constructed before 1970 (WTCB, 2005), and typically do not comprise any insulation in the building envelope. Consequently, deep energy renovation and refurbishment has become essential to hit the target by 2020.

To verify whether the thermal performance of a building envelope meets the requirements, or to determine where renovation is necessary, the as-built state has to be evaluated. To this end, it is generally accepted to consider the thermal transmittance (U-value). This value can be calculated for steady-state conditions from technical standards (EN673, 1997, ISO6946, 2007) or be measured on site by means of heat flux sensors (ISO9869(E), 1994). The latter technique determines the U-value of a building element by measuring the heat flux on one side and the surface temperature on both sides. It is important to collect data during a considerable time span (preferably about 2 weeks) as in reality the boundary conditions are always fluctuating. With a substantial dataset it is typically possible to derive a precise U-value. This method is time consuming, and in principle different points on the wall should be analysed to exclude singularities, which renders this approach rather elaborate. Infrared

thermography (IRT) could potentially improve the efficiency of on-site U-value determination. The duration of the measurement procedure with a thermographic camera is short, and this technique allows to analyze the surface temperature of a whole building part at once. In this way a more complete overview of the heat flows of a building is attained, which is a clear advantage over the point wise data of the existing methods. Evidently, the instantaneous measurement only yields a single value in time, thereby limiting its applicability and accuracy.

Nowadays, IRT is a popular tool for qualitative building diagnostics (Lucchi, 2011, Kalamees, 2007, Straube and Burnett, 1999, Burn and Schuyler, 1980, Taylor et al., 2013, Balaras and Argiriou, 2002), either for supervision of the building quality during construction or to detect defects after completion. The temperature gradients on a building surface can indicate e.g. missing or damaged insulation, air leakages or sources of moisture. More recent studies focus on *quantitative* application of IR-images: Asdrubali et al. (2012) used IRT to classify thermal bridges, other researchers tried to derive the U-value of building components (Dall'O et al., 2013, Fokaides and Kalogirou, 2011, Lehmann and Ghazi Wakili, 2013). However, this is a complex procedure due to the fact that many variable parameters influence the instantaneous surface temperature of the object, such as solar radiation, atmospheric long wave radiation, wind velocity, outside temperature fluctuation, material characteristics, indoor heating. Lehman et al. (2013) performed a sensitivity analysis for a large number of parameters on 6 different *wall* types (brick cavity wall, concrete wall, timber framed wall and 3 types of plaster-brick walls). They concluded that the external surface temperature strongly depends on the wall assembly and its thermal performance. Solar- and IR-radiation turned out to impose the strongest restrictions for quantitative IRT, because these introduce a direct temperature increment on the surface of the object. It was concluded that sunshine had to be avoided somewhere between 1 hour and 2 days before the measurements, depending on the thermal capacity and assembly of the wall.

In general, the time that is needed to reach a uniform temperature over the section of a wall is called the time constant τ , which is proportional to the square root of the thermal conductivity (λ), the density (ρ) and volumetric heat capacity (c). The larger the time constant, the more stringent the boundary conditions for IRT become in order to reduce the impact of transient effects. Windows typically have a low time constant (30min for a 4mm glass pane vs. 12h for a cavity brick wall), hence the restrictions for quantitative thermography on *glazing* are perhaps less severe. The use of IRT on windows could be a powerful application in the case of renovation or energy audits, because flux measurements on glazing units are not evident. Even a visual inspection of the thermal performance of the glass is hardly possible on site, contrary to an insulated brick wall. Next to that, IRT could have the potential to reveal degradation in time due to gas leakage.

In this paper, the investigation to suitable boundary conditions for quantitative IRT on glazing is presented. As explained before, an IR-image is a record of one moment under specific circumstances, which typically does not correspond to the steady state. A robust assessment method of the U-value should thus include a confidence interval. Six glazing types are analysed, using numerical simulations. A sensitivity analysis to internal and external climatic variations is performed.

2. Method - numerical analysis

Every object emits radiant thermal energy from its surface as long wave radiation (heat). Hence the energy received by an infrared sensor of a thermal camera consists of the emitted energy of the target. But also the surroundings emit energy, which is partially reflected by the object and in this way captured by the camera as well. Furthermore, the infrared emission of the atmosphere between the camera and the object contributes, and in the case of transparent elements, long wave radiation from behind the element is partially transmitted through and should be taken into consideration as an additional term (FIG. 1). The standard equation for incident radiation of the camera becomes:

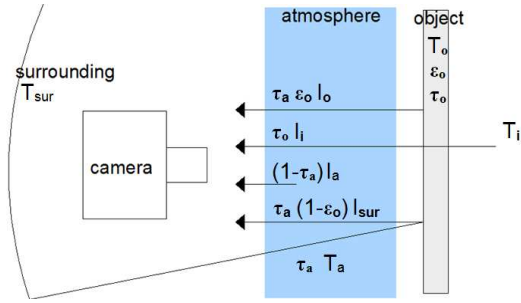


FIG. 1 Aspects of incident thermal radiation on the thermal sensor of an IR camera

$$I = \tau_a \cdot \varepsilon_o \cdot I_o^\circ + \tau_a \cdot (1 - \varepsilon_o) \cdot I_{sur} + (1 - \tau_a) \cdot I_a + \tau_o \cdot I_i \quad (1)$$

Where τ transmittance
 ε emissivity of the surface
 I irradiance
 $^\circ$ blackbody
 a, o, sur, i atmosphere, object, surroundings, interior

The incoming energy is then converted to temperature values according to the Stefan-Boltzmann law. In other words, when the parameters for atmosphere and surroundings are correctly set to the camera software, thermography allows to determine the instantaneous surface temperature of a construction (either interior (θ_{si}) or exterior (θ_{se})).

Next to that, the internal and external air temperature (θ_i and θ_e) can easily be measured on site as well. With these data and an appropriate internal or external heat transfer coefficient (h_i or h_e), the heat flux (Q) through the wall can be calculated from the wall-air temperature difference.

$$Q = h_i \cdot (\theta_i - \theta_{si}) \quad \text{or} \quad Q = h_e \cdot (\theta_e - \theta_{se}) \quad (2)$$

The heat flux can also be expressed in function of the indoor-outdoor air temperature difference,

$$Q = U \cdot (\theta_i - \theta_e) \quad (3)$$

leading to the following expression of the U-value:

$$U = h_i \cdot \left(\frac{\theta_i - \theta_{si}}{\theta_i - \theta_e} \right) = h_e \cdot \left(\frac{\theta_{se} - \theta_e}{\theta_i - \theta_e} \right) \quad [\text{W}/(\text{m}^2 \cdot \text{K})] \quad (4)$$

By definition, Eq. 4 is only valid under static boundary conditions, but it will be applied to transient conditions to assess to what extent it might provide useful information. Since the value for h_e is function of the strongly varying wind velocity (Emmel et al., 2007), this study emphasises on the determination of the U-value from the interior side. A sensitivity analysis of θ_{si} to variations in θ_i is performed by subjecting six types of windows to 3 different types of indoor temperature regimes. Additionally, the influence of the most critical outdoor parameters is analysed. Note that specific constraints in respect to thermography on glazing units are not addressed here. It is assumed that the surface temperature can be determined accurately with an IR camera. Evidently, uncertainties in emissivity and background temperature will propagate in the uncertainty interval of the estimated U-value, as well as the accuracy of the camera itself.

2.1 Cases

FIG. 2 illustrates the different glazing assemblies that are studied. These configurations are representative of those found in the Belgian building stock, and the broad variety of thermal performance levels ensures the wide applicability of the results. The properties of each layer are

derived from the European and international standards (EN673, 1997, ISO10456, 2007), and listed in TABLE 1.

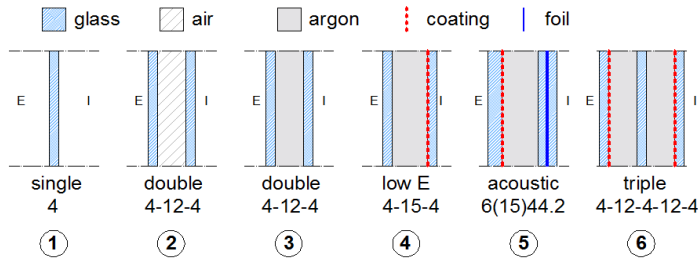


FIG. 2 Overview of the 6 investigated glazing types. Diversity in glass thickness, cavity fill and coating broadens the scope of the analysis.

TABLE 1 Properties of the 6 investigated glass types

Material Properties	t [m]	λ [W/m.K]	ρ [kg/m ³]	c [J/kg.K]	ε [-]
A Soda lime silica glass	0.004	1	2500	750	0.837
B Air	0.012	0.025	1,232	1008	-
C Argon	0.012	0.017	1.699	519	-
D Low ε -coating	-	-	-	-	0.04
E PVB-interlayer	0.0038	-	-	-	-
Glass type	Assembly (exterior - interior)		U-value ^a [W/(m ² .K)]		
1. Single Glass (Si)	A		5.75		
2. Double Glazing-air (Do+Ai)	A-B-A		2.85		
3. Double Glazing-argon (Do+Ar)	A-C-A		2.67		
4. Low E Glass (LE)	A-C (0.015m)-D-A		1.09		
5. Acoustic Glass (Ac)	A (0.006m)-D-C (0.015m)-A-E-E-A		1.08		
6. Triple Glazing (Tr)	A-D-C-A-C-D-A		0.7		

^a with standard internal and external heat transfer coefficient $h_i = 7.7$ W/(m².K) and $h_e = 25$ W/(m².K)

2.2 Simulation model

The numerical simulations are performed with the thermal analysis software VOLTRA. This program calculates transient heat transfer in 3D-objects, according to European and international standards. A solar processor takes into account of dynamic solar heat gains, based on the actual temperature and long wave radiation (Physibel, 2011).

The main purpose of the simulations is to calculate surface temperatures θ_{si} and θ_{se} , from which U-values will be deduced to evaluate the use of Equation 4 under dynamic boundary conditions. Heat transfer through conduction, convection and radiation is considered separately, according to EN 673 (1997): the radiative heat transfer is view factor based, whereas the convective heat transfer in the cavity is proportional to the Nusselt number of the gas and its thermal conductivity. The external convective heat transfer coefficient (h_{ec}) expressed in function of the wind speed (v) (Taki and Loveday, 1996), the internal convective heat transfer coefficient (h_{ic}) is calculated iteratively, using the temperature difference between the indoor air and surface (Thomas et al., 1990):

$$h_{ec} = 5.85 \cdot v^{0.52} \quad h_{ic} = 1.77 \cdot \sqrt[4]{\theta_i - \theta_{si}} \quad (5)$$

2.2.1 Outdoor boundary conditions

The simulations were carried out for a 10-days period during winter (December 17 - December 26). The meteorological data of a reference year of Uccle, Belgium was used as input. The chosen period

contains considerable variations in wind speed (v), sunny and overcast days (I_s) and variable outdoor air (θ_e) and sky (θ_{sky}) temperature, as can be seen from FIG.3.

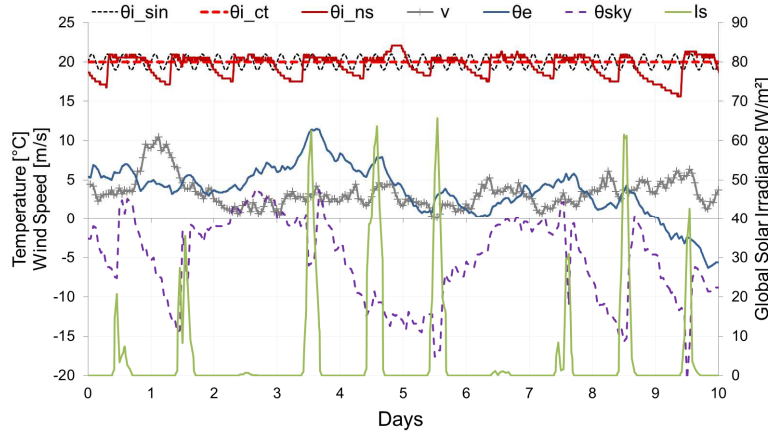


FIG. 3 Variable outdoor climate data for the period of December 17-26, Uccle, Belgium, and 3 different temperature regimes for the indoor air (0= Dec 17 0h00, 10= Dec 26 24h00)

2.2.2 Indoor boundary conditions

In this study, special attention was paid to the influence of variations in indoor air temperature. Because an IR-image shows the thermal state of a target for one specific moment, the thermal transmittance is derived by assuming these instantaneous circumstances as a steady-state condition. Nevertheless, in reality the indoor and outdoor temperatures are constantly fluctuating. To assess the effect of this assumption on the estimated U-value, simulations for each glazing assembly were carried out for 3 different indoor air temperature regimes (FIG. 3)

- θ_{i_ct} : constant temperature of 20°C
- θ_{i_sin} : fluctuating temperature $20 \pm 1^\circ\text{C}$, introduced as a sinus function with a period of 12h
- θ_{i_ns} : variable temperature with night setback (measurement data of a Belgian family house)

3. Results and discussion

3.1 Derivation of the thermal transmittance

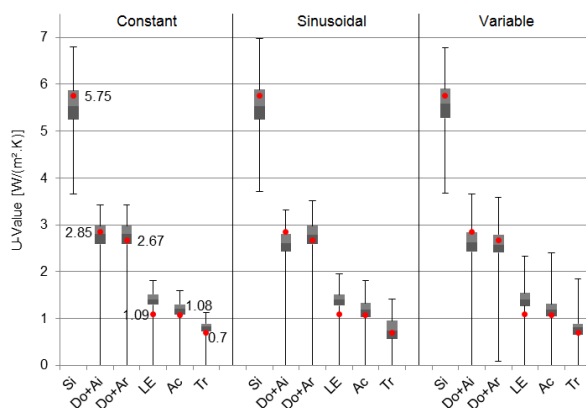


FIG. 4 U-value assessment based on θ_{si} for 3 θ_i - regimes and 6 glazing types. Note: in some cases the estimated U-value became negative, but these values are excluded from the graph.

For each indoor temperature regime, the U-value for the 6 types of glazing is estimated every 10 minutes, based on the internal surface temperature, using Equation 4 with h_i equal to $7.7 \text{ W}/(\text{m}^2.\text{K})$. In

FIG. 4 the distribution of the estimated U-value is reported. In general, it can be noticed that 50% of the assessed values (grey boxes) approximates the theoretical (red dots) thermal transmittance (an average deviation of $0.2\text{W}/(\text{m}^2\cdot\text{K})$, maximal $0.5\text{W}/(\text{m}^2\cdot\text{K})$). Even though no restrictions to the boundary conditions are made yet, this already indicates the potential of quantitative IRT on glazing. However, strongly diverging outliers (up to $4\text{W}/(\text{m}^2\cdot\text{K})$) make it impossible to rely on the result of one specific moment, neither to determine the correct type of glazing based on a single measurement without any constraints.

It can be seen that the effect of a different indoor climates only has a minor influence for less insulating windows (type 1-3). As their time constant is small enough, the surface temperature can adapt at (almost) the same frequency as the ambient air temperature. For the better insulating windows (type 4-6), the error level becomes larger, due to the higher time constant. For type 1-3, the error interval increases with about $0.2\text{W}/(\text{m}^2\cdot\text{K})$, whereas for type 4-6, it augments up to $0.8\text{W}/(\text{m}^2\cdot\text{K})$. This is especially true for glazing type 5, where the thickest glass pane is situated at the interior side.

3.2 Restrictions to the boundary conditions

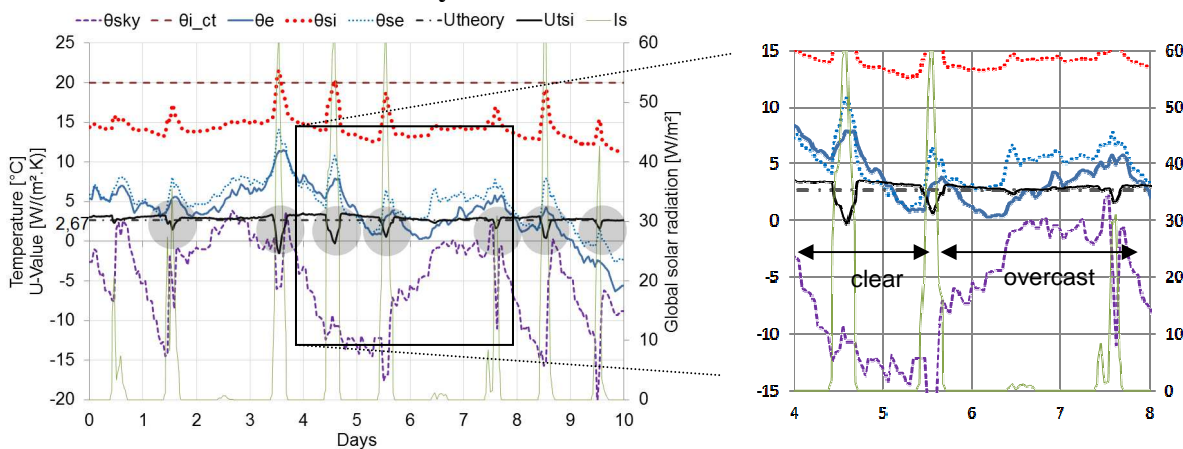


FIG. 5 Influence of the boundary conditions for the assessment of the U-value, illustrated for window type 3. During sunshine hours and clear skies, the deviation to the theoretical value increases.

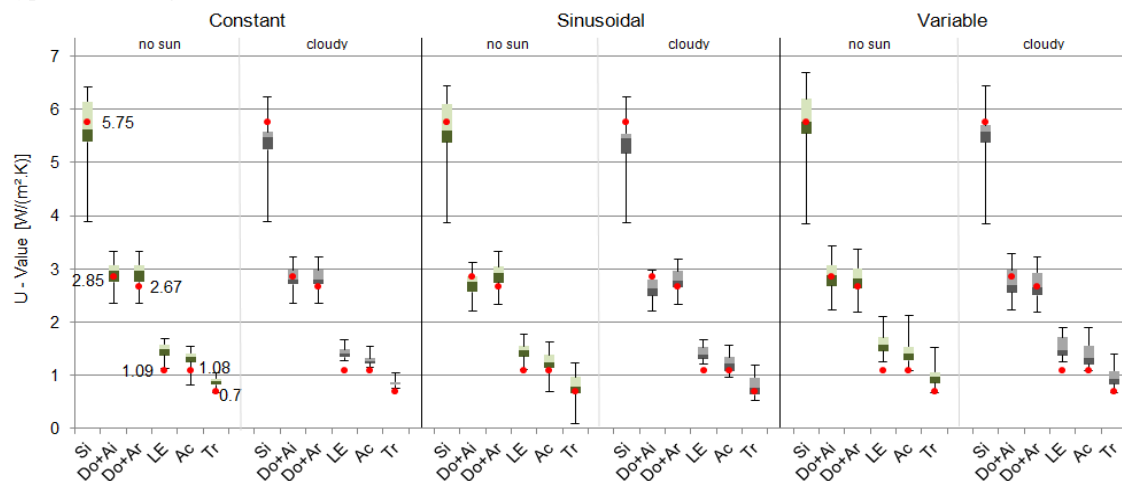


FIG. 6 Distribution of the assessed U-value (based on θ_{si}) for 3 θ_i -regimes and 6 glazing types. The results are either only excluding sunny periods (no sun) or also moments of clear sky (cloudy).

To increase the reliability of the estimation, events that cause extreme aberrations should be excluded from the data. From FIG. 5 it is clear that the largest deviations of the estimated value (U_{tsi}) come to

front in the presence of sunshine (I_s) (grey circles). Due to the *solar radiation*, the internal surface temperature (θ_{si}) of the glazing augments. It gives the impression of a better insulating quality, leading to an underestimation of the U-value. As soon as the sun disappears, this effect fades quasi instantly. Next to that, the *long wave radiation from the sky* is one of the most influencing factors. This has also been pointed out by Lehmann et al. (2013) in the case of wall assemblies. Clouds reflect the earth's long wave radiation, leading to warmer surface temperatures of exposed objects. Consequently, a clear sky corresponds to a low sky temperature (θ_{sky}), which reduces the surface temperature of the glazing and therefore leads to a higher estimated U-value (FIG.5). To assess the influence of these two outdoor parameters, the data at moments of solar radiation ($I_s \neq 0 \text{ W/m}^2$) are excluded from the U-value assessment ('no sun', FIG. 6). This roughly corresponds with the exclusion of data between 9AM and 5PM. Additionally, the data obtained during clear skies ($\theta_{sky} < -5 \text{ }^\circ\text{C}$) are also excluded ('cloudy', FIG.6).

3.3 Main findings

- The range on the results decreases substantially when direct solar radiation is avoided. Apart from single glazing, the maximal deviation from the theoretical U-value diminishes from 2.85 to 1.05 W/(m².K). It improves even more when clear sky moments are excluded, to only 0.81 W/(m².K). On average, the median deviation is only 0.24 W/(m².K), which is very accurate. Note that these values refer to the worst case scenario of internal heating pattern: night setback.
- In absence of solar radiation, this method allows to distinguish between poor insulation value (type 1), moderate insulation value (type 2, 3) and high insulation value (type 4, 5, 6).
- Assuming that the indoor temperature is kept constant, taking minor fluctuations of the heating system into account (sinusoidal regime – still realistic for on-site measurements), the U-value can be estimated with an uncertainty of at most 0.65W/(m².K) when the data is collected under the right circumstances (cloudy), except for single glazing.
- In general, the estimated U-value is systematically higher than the theoretical value. This can be attributed to a higher h_i that is used for the estimations (7.7W/(m².K)) compared to the variable value in the simulation model, which is typically depending on the type of glazing and boundary conditions and in the range of 7.0 - 7.5W/(m².K). This means that for 70 to 100% of the cases this approach yields a conservative estimation of the U-value.

4. Conclusions

This paper discusses the application of quantitative infrared thermography on window glazing. Based on numerical simulations for 6 window assemblies with different thermal performances, a sensitivity analysis has pointed out the most critical restrictions to the boundary conditions for a reliable assessment of the U-value from the interior surface temperature. Assuming that this temperature can be determined correctly, the limited simulation results show that the thermal transmittance can be estimated within a minor confidence interval of 0.65 W/(m².K) when direct sunlight and clear skies are avoided (except for single glazing). The regime of the indoor air temperature turned out to be of minor importance for the quality of the results. These findings are promising for the application of IR-thermography in assessing the insulation quality of glazing, but further research is needed to extend them to other types of windows and other periods of the year. Of course, the confidence interval will enlarge for on-site measurements because θ_{si} can only be determined within a certain range, e.g. due to the accuracy of the camera, the variability in emissivity, and the influence of the background. Future research will extend the error estimation by means of experiments, to verify the presented conclusions and include additional noise. Furthermore, the use of external surface temperatures for the assessment of the U-value will be investigated. Up to now, this data is ignored in the analysis, but including them might improve the methodology as information of both sides of the assembly is used. Also, consecutive measurements in a short time span may add to the accuracy of the U-value calculation.

5. Acknowledgements

This research is funded by the agency for Innovation by Science and Technology-Belgium (IWT), project 130210. The authors thank dr. P. Standaert for his help in the simulation modelling.

References

- ASDRUBALI, F., BALDINELLI, G. & BIANCHI, F. 2012. A quantitative methodology to evaluate thermal bridges in buildings. *Applied Energy*, 97, 365-373.
- BALARAS, C. A. & ARGIRIOU, A. A. 2002. Infrared thermography for building diagnostics. *Energy and Buildings*, 34, 171-183.
- BURN, K. & SCHUYLER, G. 1980. Applications of infrared thermography in locating and identifying building faults. *Journal of International Institute for Conservation* 4, 3-14.
- DALL'O, G., SARTO, L. & PANZA, A. 2013. Infrared Screening of Residential Buildings for Energy Audit Purposes: Results of a Field Test. *Energies*, 6, 3859-3878.
- EC 2011. Europe 2020 targets. EU EUROPEAN COMMISSION.
- EMMEL, M. G., ABADIE, M. O. & MENDES, N. 2007. New external convective heat transfer coefficient correlations for isolated low-rise buildings. *Energy and Buildings*, 39, 335-342.
- EN673 1997. Glass in building. *Determination of thermal transmittance (U value). Calculation Method*. European Standard EN.
- FOKAIDES, P. A. & KALOGIROU, S. A. 2011. Application of I thermography for the determination of the overall heat transfer coefficient in building envelopes. *Applied Energy*, 88, 4358-4365.
- ISO6946 2007. Building components and building elements. *Thermal resistance and thermal transmittance - calculation method*. ISO International Organization for Standardization
- ISO9869(E) 1994. Thermal insulation - Building elements. *In-situ measurement of thermal resistance and thermal transmittance*. International Organization for Standardization ISO.
- ISO10456 2007. Building materials and products - Hygrothermal properties - Tabulated design values and procedures for determining declared and design thermal values. ISO International Organization for Standardization.
- KALAMEES, T. 2007. Air tightness and air leakages of new lightweight single-family detached houses in Estonia. *Building and Environment*, 42, 2369-2377.
- LEHMANN, B. & GHAZI WAKILI, K. 2013. Effects of individual climatic parameters on the infrared thermography of buildings. *Applied Energy*, 110, 29-43.
- LUCCHI, E. 2011. Non-invasive method for investigating energy and environmental performances in existing buildings. *PLEA Conference on Passive and Low Energy Architecture*. Belgium.
- PHYSIBEL 2011. Voltra 7.0 Manual. Physibel Software.
- STRAUBE, J. & BURNETT, E. F. P. 1999. Rain Control and Design Strategies. *Journal of Building Physics*, 23, 41-56.
- TAKI, A. H. & LOVEDAY, D. L. 1996. External convection coefficients for framed rectangular elements on building facades. *Energy and Buildings*, 24, 147-154.
- TAYLOR, T., COUNSELL, J. & GILL, S. 2013. Energy efficiency is more than skin deep: Improving construction quality control in new-build housing using thermography. *Energy and Buildings*, 66, 222-231.
- THOMAS, F., GLANZMANN, J., KELLER, B., QUEISSER, A. & RAGONESI, M. 1990. *Element 29: Wärmeschutz im Hochbau*, Zürich, Faktor Verlag.
- WTCB 2005. Visietekst 'Bouwen en Innoveren'- Bouwen aan de toekomst. Belgisch Bouwplatform.